Geochemistry of paleokarst-hosted uranium anomalies at Abu Zarab area, southwestern Sinai, Egypt

Mahmoud Ali Gabr[1], Mohammad Hassan Awad[2], Osama Ramzy El-Shahat[2], Mohammed Abd Elhakeem Abaza[1], and Khaled Abd Elahalim[1]

[1]Nuclear Materials Authority
[2]Al-Azhar university

November 24, 2022

Abstract

Abu Zarab locality is a part from Um Bogma area in southwestern Sinai, Egypt, where paleokarsts are widespread, especially in carbonate rocks. Abu Zarab area is covered by Carboniferous carbonate rocks containing several paleokarsts. One of these paleokarsts was selected to geochemical investigation. The paleokarst was dissected by three excavated trenches constructed by Nuclear Materials Authority team to reveal its geologic features. The paleokarst is filled with lateritic components represented mainly, by gibbsite, ferruginous siltstone and clay minerals.

Twelve samples were collected from the walls of these trenches and chemically analyzed for this purpose in term of major oxides, traces and rare earth elements. The geochemical data of the major oxides display three important geochemical processes in the lateritic components of the paleokarst: (1) Enrichment of aluminum, iron and manganese; (2) depletion of calcium and magnesium (3) silicon experienced both depletion and enrichment. The geochemical data of trace and rare earth elements (REE) display enrichment of U, Cu, Pb, Zn, Ag, As and Cd with obvious enrichment of REE and conversely some elements were depleted such as V, Cr and Ga. It also, noticed that uranium has strong positive correlation with both iron and Aluminum.

This paper attempts to establish the relation between uranium and other elements in the paleokarst conditions. It is more likely, according to geochemical features of radioactive elements, that the uranium enrichment process was postdating laterite formation and the iron played an important role in capturing and trapping uranium.

Geochemistry of paleokarst-hosted uranium anomalies at Abu Zarab area,   1

southwestern Sinai, Egypt   2

[1]Awad M. H., [2]Gabr M. M., [1]Elshahat O. R., [2]Abdel Halim. A. Kh. and [2]Abaza M. M.   3

[1]Geology department, faculty of Science, Al-Azhar University, Cairo, Egypt   4

[2]Nuclear Materials Authority, P.O. Box. 530, Cairo, Egypt   5

    6

    7

Abstract: 8

Abu Zarab locality is a part from Um Bogma area in southwestern Sinai, Egypt, where paleokarsts   9
are widespread, especially in carbonate rocks. Abu Zarab area is covered by Carboniferous carbonate   10
rocks containing several paleokarsts. One of these paleokarsts was selected to geochemical   11
investigation. The paleokarst was dissected by three excavated trenches constructed by Nuclear   12
Materials Authority team to reveal its geologic features. The paleokarst is filled with lateritic   13
components represented mainly, by gibbsite, ferruginous siltstone and clay minerals.   14

Twelve samples were collected from the walls of these trenches and chemically analyzed for this   15
purpose in term of major oxides, traces and rare earth elements. The geochemical data of the major   16
oxides display three important geochemical processes in the lateritic components of the paleokarst: 17
(1) Enrichment of aluminum, iron and manganese; (2) depletion of calcium and magnesium (3) silicon   18
experienced both depletion and enrichment. The geochemical data of trace and rare earth elements   19
(REE) display enrichment of U, Cu, Pb, Zn, Ag, As and Cd with obvious enrichment of REE and   20
conversely some elements were depleted such as V, Cr and Ga. It also, noticed that uranium has   21
strong positive correlation with both iron and Aluminum.   22

This paper discusses the behavior of elements in the paleokarst and attempts to establish the   23
relation between uranium and other elements in the paleokarst conditions. It is more likely, according   24
to geochemical features of radioactive elements, that the uranium enrichment process was   25
postdating laterite formation and the iron played an important role in capturing and trapping   26
uranium.   27

    28

    29

    30

Abu Zarab is a small part from Um Bogma area which it is covered, mainly by   32

Paleozoic sedimentary succession. It had been studied by many authors (e.g. El   33

Kassas, 1967; Soliman, 1975; Mostafa, 1987; El Shahat and Kora, 1988; El- Sharkawi,   34

et al., 1990; Mansour, 1994; Botros 1995; Ashami, 1995; Aita, 1996; El Agami, 1996;   35

Abd EL-Monem, et al., 1997; Ammar et al., 1999; Afifi, 2001; Mira et al., 2006; Mira   36

and Aita, 2009; Shata and Mira, 2010; Gabr, 2013). The area is mainly covered by   37

Paleozoic succession which is represented by lower sandstone series overlies by   38

carbonate rocks (Um Bogma Formation) and upper sandstone series in the top of   39

Paleozoic succession). The carbonate rocks contains considerable amount of   40

radioactive minerals in addition to economic manganese ores. These carbonate rocks   41

contains many paleokarsts filling with lateritic materials (Bishr 2012; Aita 2012).   42

These laterite components were subjected to infinity of washing processes to   43

produce the lateritic materials in the paleokarsts. The weathering of the rocks is   44

important surficial process that leads to redistribution of elements including   45

enrichment and depletion for some elements. It is, usually controlled by many   46

factors such as climate conditions, topography, plant biological activities and parent   47

rock type (Bardossy, 1982; Bogatyrev et al., 2009). The chemical reactions during   48

lateritization processes are mainly controlled by the mineral composition of the   49

rocks and their physical properties (cleavage, porosity) which contribute in the   50

access of water to all minute grains in the mineral to be a part of reaction. The   51

second relevant factor for the formation of laterites are the properties of the   52

reacting water (dissolved constituents, temperature, acidity pH, redox potential Eh)   53

which are themselves controlled by the climate, vegetation and the morphology of   54

the landscape. Boyle (1984) mentioned that the chemical weathering slows down in   55

dry seasons at least above the fluctuating water table. The distribution of the   56

elements in paleokarst environmental   is controlled by many factors: the first   57

comprises ionic potential, Eh, pH and redox state and the second is intensity of   58

weathering which depends mainly on parent rocks, climatic conditions and the time   59

(Gay and Grandstaff, 1980; Grandstaff et al., 1986; Kimberley and Grandstaff, 1986;   60

Wronkiewicz and Condie,1987; Holland et al., 1989; McLennan, 1989; MacFarlane et   61

al., 1994; Fedo et al., 1995; Panahi et al., 2000; Mitchell and Sheldon, 2010). The ionic potential value of the element controls its behavior during the weathering processes. In other words, the elements can be divided into mobile and immobile elements according to ionic potential value during the weathering processes whereas, the element which has ionic potential value less than 3 considered mobile element because it makes weak bond with oxygen. This element prefers to release from its incorporate mineral and enters to solution during weathering processes (mobile).   In contrary, the element with higher ionic potential makes a strong bond with oxygen and it becomes resistant for weathering processes (immobile). Langmuir, (1997) proposed that some elements which have high ionic potential can form complicated oxyanions in the solution and become weakly mobile elements. Generally, aluminum, zirconium and titanium are immobile elements during the weathering processes and consider weathering resistant elements and endure stable in their minerals and finally they enriched in the karst components. Calcium, magnesium, potassium and sodium are mobile elements and they erase from their minerals to dissolve in the aqueous solution and finally depleted from the laterite components (Railsback, 2003; Sheldon and Tabor, 2009; Buggle et al., 2011). The elements Na, K, Mg and Ca do not react with other elements and are removed in the percolating water. The initial dissolution is predominantly promoted by a higher acidity (lower pH) of the water. A high percentage of the dissolved Si is equally removed but another part reacts with dissolved Al and forms the clay minerals. Si is considered mobile during alkaline condition compared to iron and aluminum (Cawsey and Mellon, 1983). Si thus obtained recombines with aluminum hydroxide formed earlier to form clay minerals. The iron and manganese behavior in karst environmental is tending to be controlled by PH and/or redox conditions.

 It should be noted that paleokarst-hosted uranium deposits Devonian-Carboniferous carbonates are an economically important new type of uranium deposits in south China (Zhu and Lin 1996).

This paper sheds some lights on the geochemical behavior of some elements, especially uranium and its relation with other elements, at Abu Zarab paleokarst

environment at Um Bogma area. Also, an attempt will be made to unravel the   92
debate concerning the origin of uranium in the carbonate rock of Um Bogma area.   93

Geological features of paleokarst   94

Abu Zarab locality is a semi-closed basin with an area of about one square   95
kilometer. It is covered by argillaceous rocks (middle member of Um Bogma   96
Formation) containing several paleokarsts. Three trenches were constructed in the   97
area by the Nuclear Materials Authority team dissecting one of these paleokarst to   98
reveal its geologic features (Fig. 1). The paleokarst is filled with zoned lateritic   99
materials represented by clay minerals, ferruginous siltstone and intercalation of   100
clay with kaolinitic components and black & white gibbsite overlies the original rock   101
of argillaceous limestone (Fig. 2).   102

103
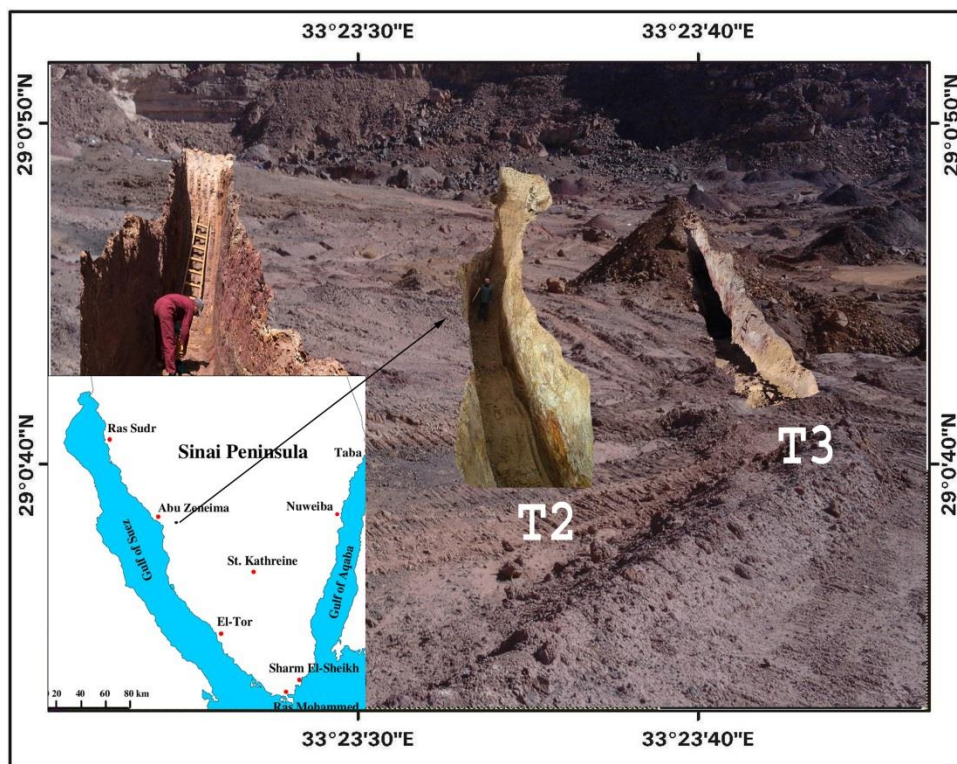
Fig. 1. Location map of Abu Zarab area   104

Sampling and analytical Techniques   105

Twelve representative samples were selected to chemical analyses. Four   106
samples from the wall of each trench marking by letters A, B, C and D. The samples   107
were taken vertically, on suitable interval from the bottom of the trench to the top.   108

The samples at the bottom started with letter D, which represented the fresh parent 109
rock (argillaceous limestone), then C, B and ended with A at the top of the wall. The 110
samples were crushed using a jaw crusher, before being powdered (95% passing 111
<100 μm) using agate rod pulverizer. The geochemical analyses of samples for 54 112
elements including Major oxides, trace and rare earth elements (REE) were carried 113
out by ACME Analytical Laboratories Ltd. (now Bureau Veritas Commodities Canada 114
Ltd.) in Vancouver, Canada using Ultra Trace by ICP-ES/MS instrument. In addition to 115
two oxides (SiO_2 and TiO_2) were analyzed in Central Laboratories of Nuclear 116
Materials Authority, Egypt. 117

The uranium radiometric measurements in the field were achieved using a 118
portable handheld gamma ray spectrometer instrument Rs-230 to reveal the 119
distribution of uranium with laterite profile in paleokarst. The radiometric works 120
started by the construction of imaginary grid with interval 0.5 meter in the vertical 121
direction and one meter in the horizontal direction on the wall of every trench. The 122
radiometric measurements data was computed using Surfer software program to 123
create contour maps. 124
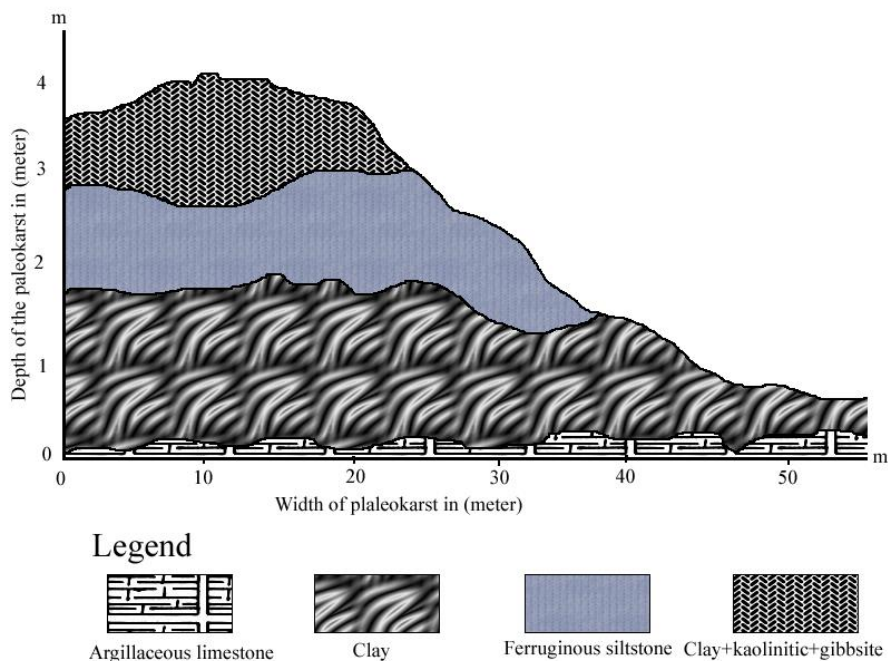
Fig. 2. Geologic diagram of paleokarst at Abu Zarab area. 127

Results and discussion

Major oxides

The chemical analyses of twelve samples for major oxides and their averages are listed in Table 1. The average of the essential elements analyses was plotted versus vertical section of laterite in paleokarst to show their curves variation (Fig.3). It gives an overview for the behavior of the major elements during the laterite evolution. SiO_2 shows two different geochemical processes from Si enrichment to desilication. The behavior of Si, in the present laterite differs from pedogenesis lateralization in most of igneous rocks that only take places in one direction. The alumina content had intensely increased with the laterite evolution and it reached to the maximum value near the surface to form black and/or white gibbsite minerals as the diagram shows. Fe has enriched with laterite evolution but it reaches the maximum value then decreases as the surface approaches. Ca, Mg and Na behavior is nearly similar whereas, they had intensely depleted with laterite evolution. Calcium and Magnesium oxides were major constituents of the argillaceous limestone but with the intensity of weathering they experienced great depletion in their contents. The calcium and magnesium contents in laterite gave an idea about the intensity of weathering and the time which the lateritic materials subjected to the weathering processes. The high weathering and long time is more depletion of calcium and magnesium contents and vice versa.

Trace elements

The trace elements contents in parent rock and laterite in paleokarst with averages are listed in Table 2. The table gives a clear conception about the behavior of the elements under lateritic conditions. The averages of some important trace element contents were plotted versus the vertical section of paleokarst to illustrate their distribution with laterite profile in paleokarst (Fig 4). The figure shows obvious enrichments in some traces and strong depletion in other trace elements while some elements have experienced alternating enrichment and depletion processes and they can be classified according to their concentrations into enriched, depleted and nearly constant elements. The enriched elements comprise Mo, Cu, Zn, Ag, Ni, Co, U,

Sr, Cd, Ba, Be, Y and Se. The depleted elements comprise As, V, Cr and Ga. The 159

nearly constant elements comprise Pb, Th, Sb, Bi, Ti, W, Zr, Sn, Sc, S, Hf, Li, Rb, Ta, 160

Nb, Cs, In, Re, Te and Tl. Copper content is very low in the parent rock but it 161

experienced high enrichment in its content in the early stage of laterite development 162

and in the last stage it displays decreasing. Lead is nearly constant in its content with 163

evolution of laterite with slightly enrichment in the last stage of evolution. Five 164

elements (Zn, Ni, Co, Ba, Cd) have nearly similar behavior to copper whereas all of 165

them experienced high enrichment in the early stage then decreasing in their 166

contents in the finally stage of laterite evolution. Strontium content is very low in the 167

parent rock then enriched in the first stage of laterite evolution then experienced 168

high decreasing in its content with more development then it had enriched to reach 169

the maximum value in the end stage of evolution. Vanadium and chromium 170

behaviors are nearly similar with slightly differences whereas their contents are high 171

in the parent rock but they decreased with evolution of the laterite. 172

Table 1. Chemical analyses of major oxides (Wt. %) and averages for the paleokarst. 173

	SiO_2	TiO2	Al_2O_3	Fe_2O_3	MnO	MgO	CaO	Na_2O	K_2O	P_2O_5
1D	38.2	0.39	4.7	5.19	0.02	2.66	19.88	1.24	0.37	0.16
2D	37.1	0.46	6.12	3.32	0.01	6.28	17.18	1.39	0.59	0.17
3D	34.61	0.83	4..3	4.55	0.12	3.35	11.2	1.61	0.81	0.13
average	36.64	0.56	5.41	4.35	0.05	4.10	16.09	1.41	0.59	0.15
1C	30.8	0.18	11.34	12.68	1.3	0.88	0.48	1.2	1.37	0.07
2C	29.9	0.19	11.71	12.24	1.3	0.96	0.49	1.21	1.4	0.06
3C	28.8	0.2	11.53	11.61	>1.3	1.04	0.55	1.22	1.53	0.07
average	29.83	0.19	11.53	12.18	1.30	0.96	0.51	1.21	1.43	0.07
1B	44.35	0.64	13.85	28.88	0.09	0.71	0.29	0.77	1.31	0.11
2B	45.3	0.71	15.13	26.16	0.07	0.38	0.39	0.84	1.46	0.08
3B	43.8	0.78	17.25	30.6	0.09	0.28	0.15	0.49	0.95	0.12
average	44.48	0.71	15.41	28.55	0.08	0.46	0.28	0.70	1.24	0.10
1A	29.8	1.1	17.61	12.36	0.12	0.85	1.02	0.55	2.01	0.15
2A	28.9	0.9	16.08	10.81	0.06	1.11	1.13	0.68	2.25	0.17
3A	26.4	0.8	16.84	12.17	0.12	0.96	1.08	0.59	1.9	0.16
average	28.37	0.93	16.84	11.78	0.10	0.97	1.08	0.61	2.05	0.16

174

Rare earth elements (REE) 175

The results of chemical analyses of (REE) for parent rock and laterite with some 176

geochemical parameters are presented in Table 3. The sum of REE content of laterite 177

is more than the REE content of the parent rocks pointing to enrichment of REE in 178

the laterite. The LREE/HREE ratio ranges between 2.49 and 8.85. The chondrite-normalized distribution pattern is shown in figure 5. It displays similarity in distribution pattern of REE between the parent rock and laterite which are characterized by LREE enrichment more than HREE with small negative Eu for either parent rock or laterite samples.

In conclusion: the geochemical behavior of elements in paleokarst points to three stages during laterite evolution. The first stage characterized by strongly leaching of Si, Ca, Mg and Na while Al and Fe are enriched. Also it is experienced depleted in Cr and V but Cu, Zn, Co, Ni, Sr, Ba and Cd are enriched while, the REE are strongly enriched. The second stage characterized by enrichment of Si, Al and Fe but Ca, Mg and Na are depleted while Cu, pb, Zn, Ni, Co, Sr, Cd and Ba are depleted but V and Cr are enriched. The third stage is experienced depletion in Si and Fe but Al is enriched while Ca and Mg are slightly enriched with nearly constant concentration of Na. Cu and Zn are depleted while Pb, Co, V, Sr and Ba are enriched but Ni, Cr and Cd are nearly constant.

The samples which were taken from clay zone show high content of REE and that is comfortable with the study of Condie et al., (1995). He proposed that REE is preferred to be adsorbed on clays during weathering processes.

Uranium in karst

The radiometric contour maps for trenches (1, 2 and 3) are shown in the figures (6A,B,C), respectively. The figures show high uranium contents in the majority of walls of the three trenches ranging from 100 ppm to more than 500 ppm. The high anomalies of uranium are hosted in ferruginous siltstone but also clay zone hosts considerable amount of uranium.

The correlation coefficient values of uranium versus some other elements are listed in Table 4. It shows strong positive correlation between uranium versus Fe_2O_3, Th, SiO_2 and Al_2O_3 while it has negative correlation with Mg, CaO and Na_2O. The highest correlation coefficient value is found between uranium and Fe_2O_3 (0.98) which gives indication that there is a positive relation between iron oxide and enrichment of uranium in laterite. The geochemical of uranium and thorium data were plotted

versus vertical section of laterite to create variation diagram (Fig. 7). The figure 209
shows strong enrichment of uranium but weakly enrichment for thorium with 210
laterite evolution and uranium reached to its maximum content in ferruginous 211
siltstone then decreased in gibbsite zone near the surface. 212
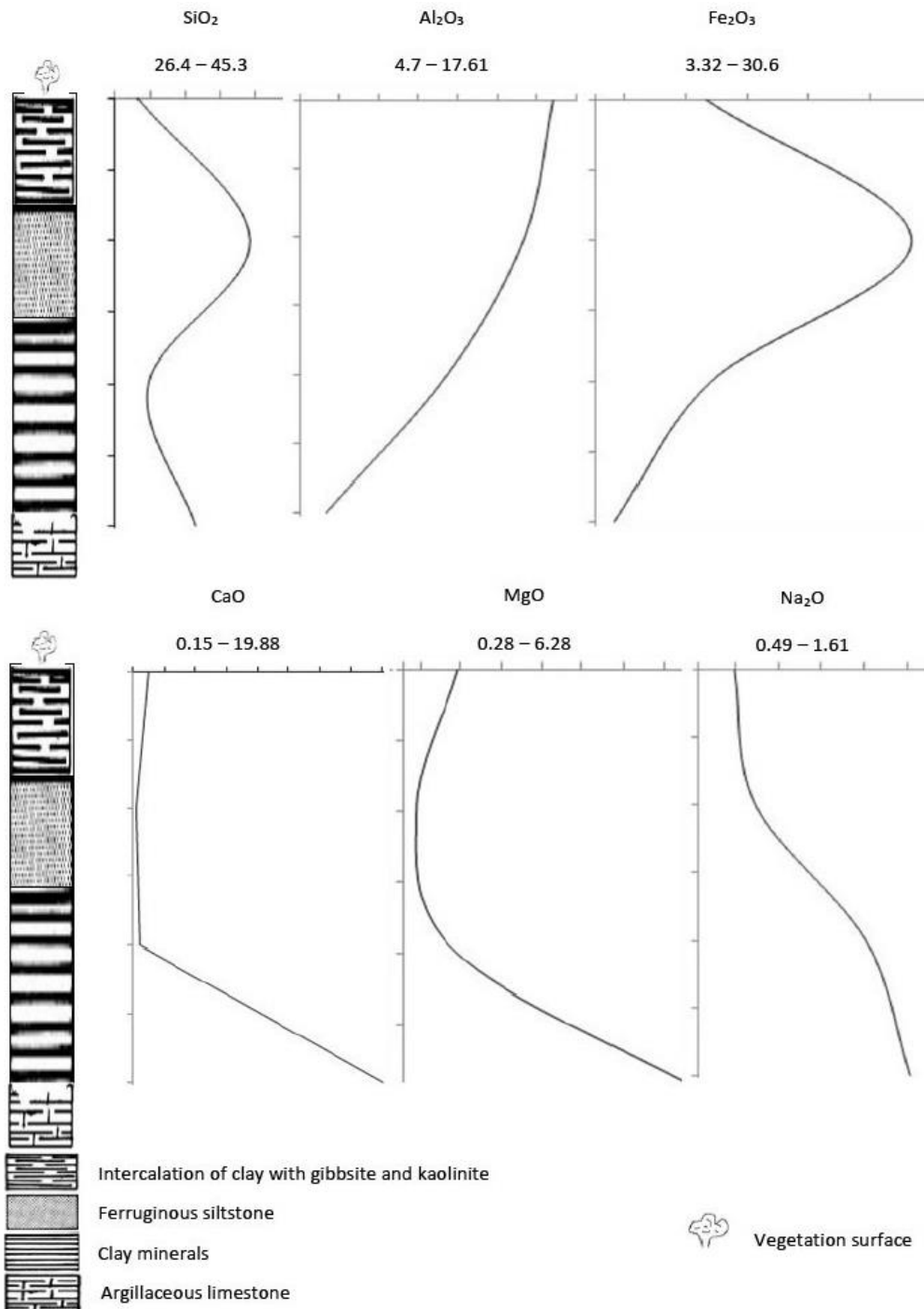
Fig.3. Variation curves for the major oxide contents (%) vs depth of laterite (m) 215

Origin of uranium   217

   Three concepts for the origin of uranium occurrence in the area can be discussed,   218
the first assumes that uranium is deposited contemporaneously with the deposition   219
of carbonate rocks (syngenetic) but this concept is inconsistent with field radiometric   220
survey, as no extension of uranium anomalies had been recorded with fresh   221
carbonate rocks, but the majority of uranium anomalies are confined with   222
paleokarsts. Moreover, the carbonate rocks are generally, considered from the least   223
uraniferous rocks between the earth crust according to chemical analyses of many   224
samples in many literatures of Um Bogma area, south Sinai and other areas around   225
the world (e.g. Ashami, 1995; Aita, 1996; El Agami, 1996; Afifi, 2001; El Aassy, et al.,   226
2006; Gabr 2013). Bell (1963) mentioned that the rocks which composed wholly of   227
carbonate minerals and that include only minute traces of other constituents   228
generally contain about 1 ppm or less, of syngenetically deposited uranium; they are   229
among the least uraniferous rocks.   230

   The second concept is that uranium has been enriched during the evolution of the   231
laterite, but the geochemical environment of the laterite formation usually take   232
place in surficial intensive weathering under oxidation conditions and these   233
conditions is not suitable for uranium deposition whereas, the uranium is mobile   234
element in the oxidation condition (Finch and Murakami, 1999).   235

   The third concept proposed uranium precipitation postdating filling up of the   236
paleokarast by lateritic materials (epigenetic). This concept is most likely accepted to   237
interpret the origin of uranium in the studied paleokarast. The studied paleokarast is   238
filled up with lateritic materials such as clay, ferruginous siltstone, intercalation of   239
clay with kaolinitic components and black & white gibbsite. These materials can   240
adsorb the uranium from circulating solutions and considered as good favorable trap   241
for uranium.   242

   Many authors interpreted the occurrence of uranium anomalies in laterite (e.g.   243
Gritsaienko, et al., 1958; Sharkov and Yakoleva 1971). They ascribed the origin of   244
uranium in laterite to two physic-chemical processes responsible for precipitation of   245
uranium in laterite. The first is co-precipitation, in this case the iron and uranium   246
hydroxides can precipitate from acidic sulphate solutions by neutralization but this   247

process is common with high grade of uranium >0.1% but the studied uranium is low

grade (less than 0.1%).

Table 2. Chemical analyses of trace elements (ppm& Ag in ppb) for the studied paleokarst

	Mo	Cu	Pb	Zn	Ag	Ni	Co	As	U	Th
1D	85	211.3	213.25	270	ud	468.3	31.83	470	31.5	13.5
2D	87	186	114.36	196.4	ud	384.2	29.1	366	21.1	11.9
3D	61	124	287.59	311.2	ud	288.6	208.3	247	11.7	4.5
average	77.67	173.77	205.07	259.20	-	380.37	89.74	361.00	21.43	9.97
1C	90.65	>10000.0	204.1	>10000.0	4086	1299.8	1501.7	158.2	281.9	12.5
2C	101.11	>10000.0	266.1	>10000.0	4438	1301.7	1550.4	158.2	253.5	12.2
3C	88.12	>10000.0	189.3	>10000.0	3941	1101.2	1391.7	158.2	230.1	11.1
average	93.29	>10000	219.83	>10000	4155.00	1234.23	1481.27	158.20	255.17	11.93
1B	116.06	6299.9	196.09	3926.8	609	208.3	70.7	310.8	974.9	18.5
2B	130.1	7102.1	203.14	4122.1	671	290.1	77.3	290.3	730.2	17
3B	110.02	4235.6	187.3	3870.2	701	211.2	89.2	403.2	988.1	23.5
average	118.73	5879.20	195.51	3973.03	660.33	236.53	79.07	334.77	897.73	19.67
1A	144.54	3178	248.35	1761.9	574	156.1	117.1	277.7	153.9	16.3
2A	204.07	2988.4	291.21	1150.7	538	118.3	121.6	249.6	144.6	14.2
3A	95.63	3187.9	312.75	2130.5	477	161.4	119.1	269.9	151.2	14.8
average	148.08	3118.10	284.10	1681.03	529.67	145.27	119.27	265.73	149.90	15.10

ud = undetected

detection limit is 20 ppb for Ag

Table 2. Continued

	Sr	Cd	Sb	Bi	V	Cr	Ba	Ti	W	Zr	Sn
1D	63	10.22	6.21	0.12	766	409.1	183	0.231	0.3	148	1.7
2D	76	13.54	5.37	0.13	680	436.7	162	0.232	0.4	214	1.1
3D	45	6.8	9.11	0.12	634	386.2	127	0.237	0.6	137	1.4
average	61.33	10.19	6.90	0.12	693.33	410.67	157.33	0.23	0.43	166.33	1.40
1C	449	188.63	4.41	0.16	225	162	652	0.327	0.6	208.7	2.7
2C	451	192.22	3.81	0.17	277	128	563	0.211	0.3	213.4	2.3
3C	398	201.51	4.02	0.16	231	184	710	0.361	0.8	188.1	2.3
average	432.67	194.12	4.08	0.16	244.33	158.00	641.67	0.30	0.57	203.40	2.43
1B	137	27.99	6.41	0.31	240	209	82	0.323	0.6	161	2
2B	204	19.3	5.21	0.11	290	310	83	0.299	0.3	209	3
3B	113	36.7	11.3	0.38	202	196	64	0.311	0.8	286	2
average	151.33	28.00	7.64	0.27	244.00	238.33	76.33	0.31	0.57	218.67	2.33
1A	609	13.62	9.64	0.29	319	219	177	0.371	0.6	197.4	2.4
2A	588	12.88	11.11	0.18	370	310	181	0.364	0.5	117.3	2.5
3A	603	13.43	9.86	0.21	315	214	178	0.346	0.6	197.2	2.4
average	600.00	13.31	10.20	0.23	334.67	247.67	178.67	0.36	0.57	170.63	2.43

Table 2. Continued   256

	Be	Sc	S	Y	Hf	Li	Rb	Ta	Nb	Cs	Ga
1D	18	16.9	0.22	17	0.71	13.4	48	1.2	35.81	3.2	222.3
2D	11	12.9	0.07	28	2.31	17.2	51	1.2	41.2	2.7	241.7
3D	8	9.9	0.19	14	0.64	19.3	39	1.1	19.7	1.9	198.8
average	12.33	13.23	0.16	19.67	1.22	16.63	46.00	1.17	32.24	2.60	220.93
1C	61	8.6	0.24	494.2	5.54	9.2	46.8	1.9	31.21	7.1	16.72
2C	68	8.9	0.28	503.1	5.41	11.3	38.1	1.2	25.6	6.8	17.82
3C	81	6.8	0.22	444.8	4.61	7.2	51.9	1.3	32.41	6.4	14.23
average	70.00	8.10	0.25	480.70	5.19	9.23	45.60	1.47	29.74	6.77	16.26
1B	59	18.1	0.13	183.5	4.52	9	39.1	1.5	21.07	6.1	14.49
2B	66	21.1	0.17	129.1	8.5	7	47.3	2.1	27.05	4.3	13.55
3B	42	17.5	0.17	214.9	9.11	11	32.5	2.2	22.01	6.2	21.66
average	55.67	18.90	0.16	175.83	7.38	9.00	39.63	1.93	23.38	5.53	16.57
1A	25	15.6	1.31	76.2	5.53	19.4	50.7	1.9	31.02	6.9	16.17
2A	29	12.7	1.28	81.3	4.2	17.1	81.2	1.8	29.14	5.8	19.21
3A	27	14.3	1.31	78.6	5.42	20.6	52.3	1.9	30.82	6.8	15.29
average	27.00	14.20	1.30	78.70	5.05	19.03	61.40	1.87	30.33	6.50	16.89

The second process most likely interprets the origin of uranium in the studied   258
paleokarst. It is surface adsorption process comprising both sorption and   259
precipitation on active surfaces. The sorption process occurs when ions are   260
attracted to mineral surfaces has opposite electrical charges. The ability of mineral   261
faces to attract or adsorb ions from its solution differs from mineral to the other. The 262
ability of mineral is measured by the quantity of adsorbed uranium on its faces by   263
the residual quantity in solution and this ratio is known as geochemical enrichment   264
factor GEF. Langmuir, (1978) proposed geochemical enrichment factors (GEF) of   265
uranium for some natural sorbents (Table 5). The sorption of uranil ions on iron   266
oxide hydroxide species is responsible for distribution of uranium in iron-rich   267
geochemical terrains (Barton, 1956; Rojkova, et al., 1958; Van Der Veijden, et al.,   268
1974; Zhmodik, et al., 1980; Michel, 1983).   269

   In conclusion, the paleokarst is formed then it is filled with rock fragments in   270
tropic to semi-tropic conditions. The rock fragments subjected to intensive   271
weathering processes led to laterite formation in the paleokarst. It is filled with   272
lateritic materials which enrich in iron and aluminum oxides with many other   273
elements. The paleokarst components are considered good trap for dissolved   274
uranium. The iron oxides play a main role in capturing uranium by surface adsorption   275

process. The uranium in the area is considered supergene low grade ore and   276
concentrated later the end of lateritic process inside the paleokarst.   277

278
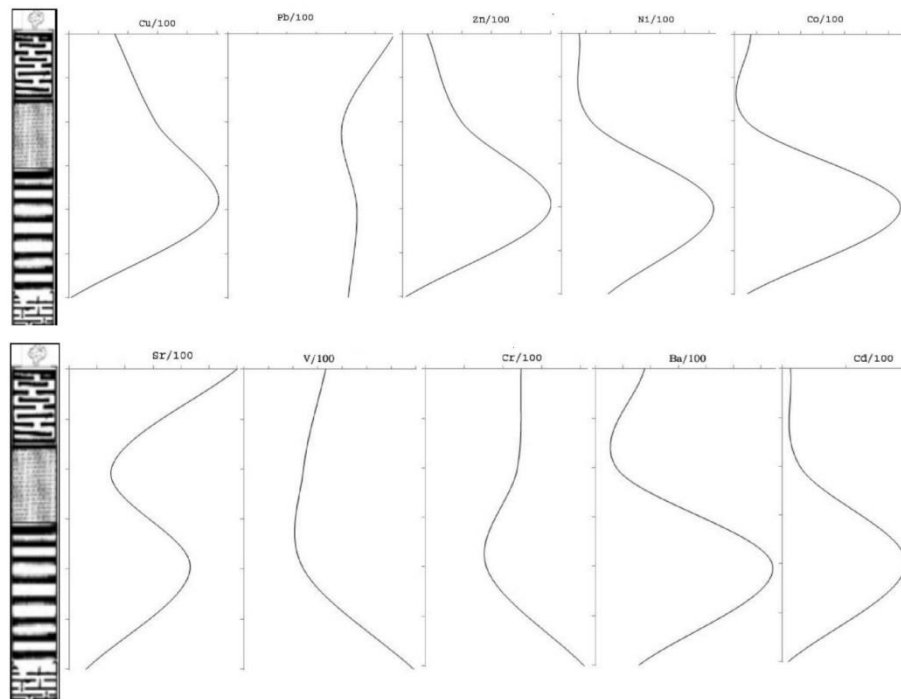
Fig.4. Variation curves for some trace element contents (ppm) vs depth of laterite   279

Symbols as figure 3   280

Summary and conclusion   281

Um Bogma area localizes in southwestern Sinai, Egypt. It is covered mainly by   282
Paleozoic sedimentary rocks. It is one of the dominating paleokarst regions, where   283
laterite is widespread. A paleokarst at Abu Zarab locality hosting uranium which   284
belongs to um Bogma area was selected for this study. Three trenches were   285
constructed in the paleokarst to reveal their lithostratigraphy and uranium   286
distribution along vertical sections cross cutting the paleokarst. The geology of the   287
trenches is arranged beginning with the oldest as follows a) argillaceous limestone,   288
b) clay minerals, c) ferruginous siltstone and d) intercalation of clay with kaolinitic   289
components and black & white gibbsite. The geochemical data of the major oxides   290
display three important geochemical processes in the lateritic components of the   291
paleokarst. (1) Enrichment of aluminum, iron and manganese; (2) depletion of   292
calcium and magnesium (3) silicon experienced both depletion and enrichment. The   293
geochemical data of trace and rare earth elements (REE) display enrichment of Cu,   294

Pb, Zn, Ag, U, As and Cd with obvious enrichment of REE. It also, noticed that 295

uranium has strong positive correlation with both iron and Aluminum. It is more 296

likely, according to geochemical features of radioactive elements that the uranium 297

was enriched later than formation of laterite. The iron played an important role in 298

capturing and trapping the uranium. 299

Table 3. Chemical analyses of REE (ppm) for the studied paleokarst. 300

	La	Ce	Pr	Nd	Sm	Eu	Gd	Tb	Dy	Ho	Er	Tm	Yb	Lu	ΣREE	ΣLREE	ΣHR
1D	7.1	15.22	2.2	16.3	6.3	2.3	11.5	1.2	5.3	0.7	2.2	0.3	1.4	0.1	72.12	60.92	11
2D	18.3	21.5	3.4	31.6	7.9	3.3	17.2	2.7	6.9	1.1	3.5	0.9	2.8	0.2	121.3	103.2	18
3D	11.5	18.4	2.8	29.4	5.6	1.9	10.9	2.1	5.5	0.9	2.7	0.4	1.8	0.2	94.1	80.5	13
1C	77.4	206.01	38.3	249.7	114.6	27.9	192.4	27.3	128.9	21.3	47	4.9	24.2	3.4	1163.3	906.31	25
2C	69.1	188.5	34.8	211.2	107.2	22.7	181.4	22.4	109.4	19.4	36	3.8	21.9	2.5	1030.3	814.9	215
3C	73.8	201.2	41.2	230.5	109.2	21.6	188.6	26.5	127.9	21.1	47	3.9	23.8	3.1	1119.4	866.1	253
1B	63.6	107.03	20.3	115.3	55.1	14.5	76.3	13.2	65.3	10.7	25.5	3.4	18.5	2.6	591.33	452.13	139
2B	55.7	117.08	18.9	110.7	44.6	11.5	48.2	11.5	48.5	8.1	11.8	3.8	11.5	3.6	505.48	406.68	98
3B	93.1	113.06	29.8	127.1	55.1	19.3	89.7	17.5	91.5	18.9	37.9	6.7	31.5	7.8	738.96	527.16	211
1A	84.9	150.65	27.3	106.1	27.2	6.1	29.5	4.7	23.4	4.2	10	1.4	7.7	1.1	484.25	431.75	52
2A	77.5	144.66	18.6	110.5	24.6	4.8	22.9	3.8	21.1	3.9	8.1	1.7	6.1	0.9	449.16	403.56	45
3A	85	152.37	26.5	106.6	26.4	5.7	28	4.4	24	3.8	9.3	1.3	7	1.1	481.47	430.57	50

301
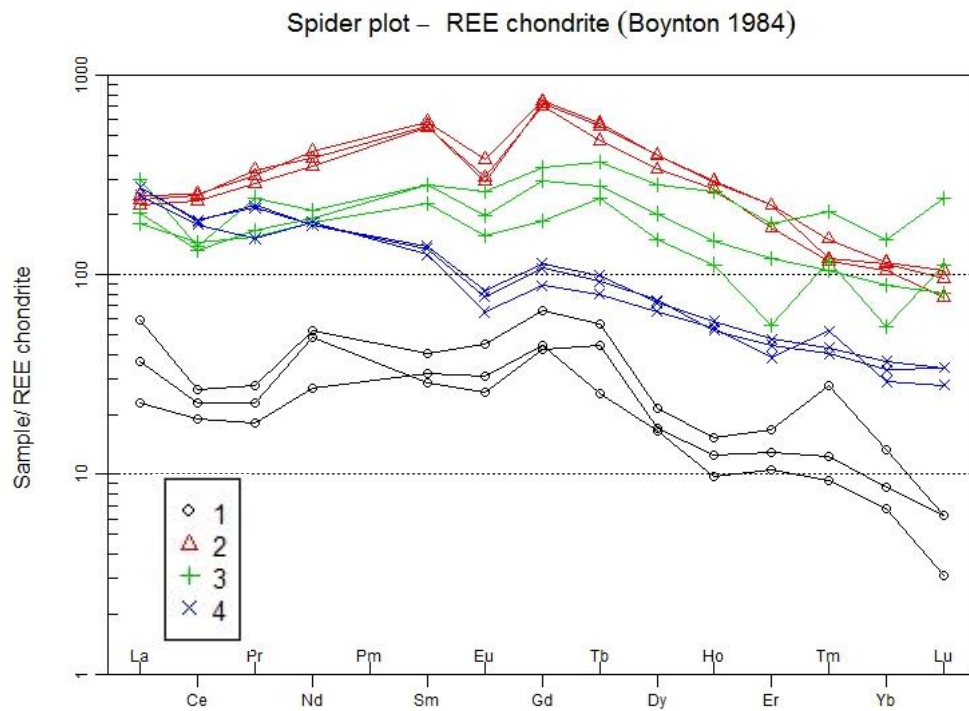

Fig. 5. Normalized pattern of the studied REE 303

1= argillaceous limestone   2 = clay minerals   3= ferruginous siltstone   4= clay+gibbsite+kaolenite 304

305
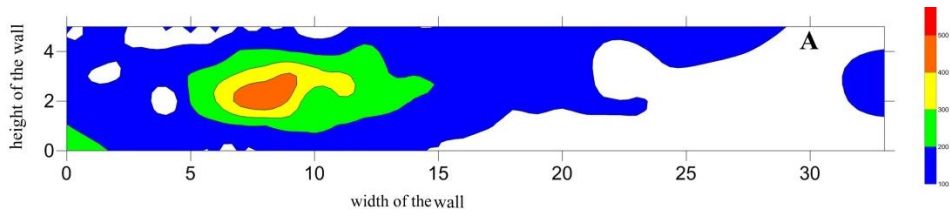
306
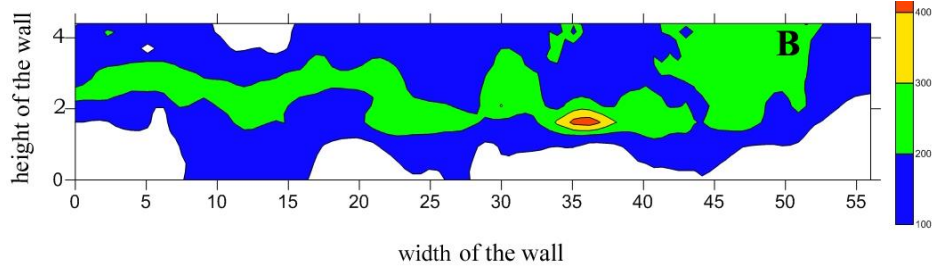
307
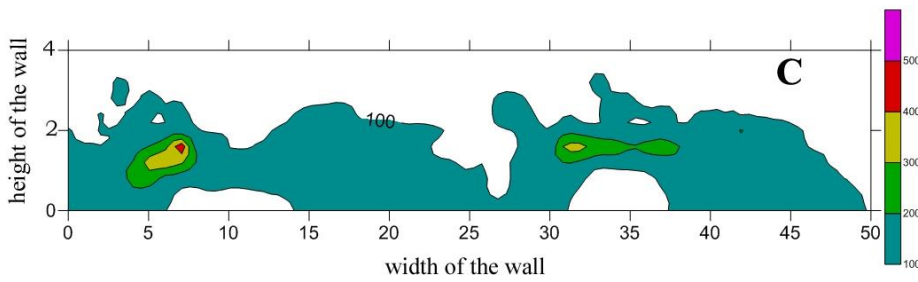
308

Fig.6,A,B,C. Contour maps for distribution of uranium content in the walls of trenches (1,2,3)   309

Table 4. Correlation coefficient values of uranium (ppm) with major oxides (%).   310

	SiO_2	Th	TiO2	Al_2O_3	Fe_2O_3	MnO	MgO	CaO	Na_2O	K_2O	P_2O_5
Correlation Co. with U	0.72	0.78	0.11	0.45	0.98	0.18	-0.56	-0.53	-0.52	0.02	-0.38
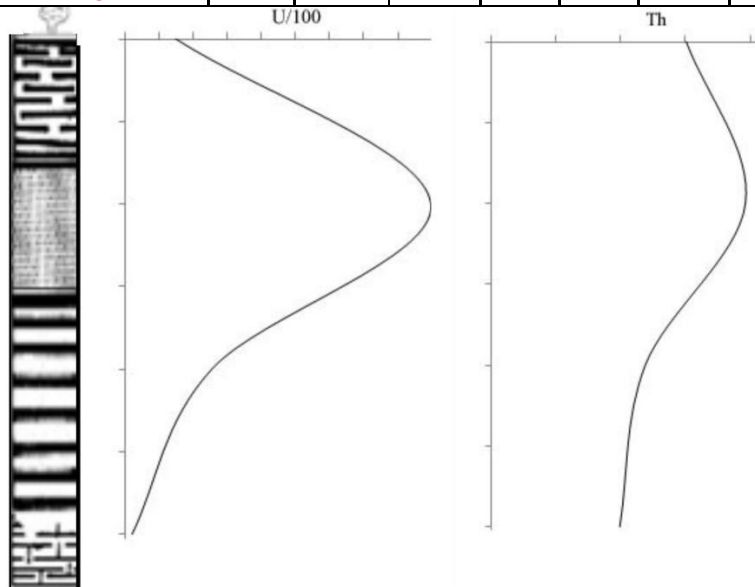
311

Fig.7. Variation curves for U and Th element contents (ppm) vs. laterite section.   312

Symbols as figure 3   313

Table 5. Geochemical enrichment factor (GEF) for some natural surbents (Langmuir, 1987)

Mineral Sorbents	GEF
amorphous $Fe(OH)_3$	$1.1 \times 10^6 - 2.7 \times 10^6$
fine-grained goethite	4×10^3
amorphous $Ti(OH)_4$	$8 \times 10^4 - 10^6$
phosphorites	15
montmorillonite	6
kaolinite	2

References

Abd EL-Monem, A., El-Aaassy, I.E., Hegab, O., EL-Fayomy, I., and EL-Agami, N., (1997): Gibbsite uranium and copper mineralization, Um Bogma area, south western Sinai, Egypt sedimentology of Egypt , 5, 117-132.

Afifi, S.Y., (2001): Paragenesis of Mn-Cu-U in Quaternary paleochannels, West Central Sinai, Egypt. 5th Inter. Conf. On Geochemistry. Alex. Univ. Egypt, 12-13.

Aita, S.K., (1996): Geological, mineralogical and geochemical studies on some radioactive anomalies of the Paleozoic sediments of Um Bogma area, West Central Sinai Egypt, M.Sc. Thesis, Faculty of Science, Cairo University, 262 p.

Aita, S.K., (2012): Bioleaching of Uranium - bearing material from Abu Thor area, West Central Sinai, Egypt for recovering uranium. Arab Journal of Nuclear Sci. and Appl., 45(2)169-178

Ammar, F.A., Abdou, N.M.F., and Dewedar A.A., (1999): Mineralogy and Geochemistry of the Radioactive shale bed of the middle Member of Um Bogma Formation in Allouga Exploratory Tunnels, West central Sinai, Egypt. 4th intern. Conf. On Geochemistry , Alex. Univ., Egypt, 15-16 Sept., 1999, 179-198.

Ashami, A.S., (1995): Studies on geology and uranium occurrences of some Paleozoic rocks, Wadi Allouga area, Sinai, Egypt. M.Sc. Thesis, Faculty of Science, Zagazig University, 156 p.

Bardossy, G., (1982): Karst Bauxites (bauxite deposits on carbonate rocks). Developments in Economic Geology, 14, 401–441.

Barton, P.B., (1956): Fixation of uranium in the oxidized base metal ores of the Goodsprings District Clark Co. Nevada, Econ. Geol., 51, 178-191.

Bell, K.G., (1963): Uranium in carbonate rocks, Geological Survey, U.S.A. Professional paper, 474-a

Bishr. H. A., (2012): Primary uranium mineralization in paleochannels of the Um Bogma Formation at Allouga, Southwestern Sinai, Egypt. Eleventh Arab Conference on the Peaceful Uses of Atomic Energy, Khartoum, Sudan: 23-27 Dec. 2012, 1-12.

Bogatyrev, B.A., Zhukov, V.V. and Tsekhovsky, Y.G., (2009): Formation conditions and regularities of the distribution of large and superlarge bauxite deposits. Lithology and Mineral Research, 44, No. 2, 135–151.

Botros, N., (1995): The effect of rift tectonics on the mode of distribution of uranium bearing sediments, Um Bogma area, West Central Sinai, Egypt. Ascad. Sci., 45, 193- 204.

Boyle, D.R., (1984): The genesis of surficial uranium deposits. In: TOEN, P.D. (ed) Surficial Uranium Deposits. IAEA-Tecdoc-322. Vienna, 45-52.

Buggle, B., Glaser, B., Hambach, U., Gerasimenko, N. and Markovi_C, S., (2011): An evaluation of geochemical weathering indices in loess e paleosol studies. Quaternary International, 240, 12-21.

Cawsey, D.C. and Melon, P., (1983): A review of experimental weathering of basic igneous rocks. Geological Society London, 11(1):19-24

Condie, K.C., Dengate, J., Cullers, R.L., (1995): Behaviour of rare earth elements in the paleoweathering profile on granodiorite in the Front Range, Colorado, USA. Geochimica et Cosmochimica Acta, 59, 279-294.

El Aassy, I.E., Ahmed, F.Y., Al Shami, A.S., Shata, A.E., Gabr, M.M. and Rizq, A.A., (2006): Geochemical differentiation of REE in karst laterites, Sinai, Egypt: 7th Inter. Conf. Geochem., Fac. Sci., Alex. Univ., Alex., Egypt, II, 75-81.

367

El Agami, N.L., (1996): Geology and radioactivity studies on the Paleozoic rock units in the Sinai Peninsula, Egypt. Ph.D. Thesis, Fac. of Science, Mansoura Univ., Egypt, 302p.

El Kassas, I.A., (1967): Geologic and radiometric prospection of radioactive raw materials in West Central Sinai, Internal Report, geology and Raw Materials Dept. (AEE), Cairo.

EL Shahat, A. and Kora, M., (1988): Composition of dolostones of Um Bogma Formation, Sinai, Mansoura science Bulletin, 15, 33-58.

El Sharkawi, M.A., El-Aref, and Abdel Motelib, A., (1990): Manganese deposits in a Carboniferous paleokarst profile, Um Bogma region, West Central Sinai, Egypt. Mineralium Deposita, 25, 323-343.

Fedo, C.M., Nesbitt, H.W., Young, G.M., (1995): Unravelling the effects of potassium metasomatism in sedimentary rocks and paleosols, with implications for paleoweathering conditions and provenance. Geology, 23, 921-924.

Finch, R. and Murakami, T., (1999): Systematics and paragenesis of uranium minerals. In: Uranium: Mineralogy, Geochemistry and the Environment (Eds. BURNS, P.C. and FINCH, R.). Reviews in Mineralogy, 38, 91-180.

Gabr, M. M., (2013): Structural control of uranium and associated elements in the area around Wadi Sad Banat, Southwestern Sinai, Egypt. Sedimentology of Egypt, 21, 207-220.

Gay, A.L., Grandstaff, D.E., (1980): Chemistry and mineralogy of Precambrian paleosols of Elliot Lake, Ontario, Canada. Precambrian Research, 12, 349-373.

Grandstaff, D.E., Edelman, M.J., Foster, R.W., Zbinden, E., Kimberley, M.M., (1986): Chemistry and mineralogy of the Precambrian paleosols at the base of the Dominion and Pongola Groups (Transvaal, South Africa). Precambrian Research, 32, 97-132.

Gritsaienko, G.S., Belova, L.N., Getseva, R.V. and Sayelyeva, K.T., (1958): Mineralogical types of oxidation zones of hydrothermal uranium and sulfide uranium ores of the USSR, UN Intern. Conf. Peaceful Uses of Atomic Energy Proc., 2, 469-471.

Holland, H.D., Feakes, C.R., Zbinden, E.A., (1989): The Flin Flon paleosol and the composition of the atmosphere 1.8 BYBP. Science, 289, 362-389.

Kimberley, M.M., Grandstaff, D.E., (1986): Profiles of elemental concentrations in Precambrian paleosols on basaltic and granitic parent materials. Precambrian Research, 32, 133-154.

Langmuir, D., (1978): Uranium solution-mineral equilibria at low temperature with application to sedimentary ore deposits, Geochim Cosmochim. Acta. 42, 547-569.

Langmuir, D., (1997): Aqueous Environmental Geochemistry. Prentice Hall, New Jersey, USA, 600 p.

MacFarlane, A.W., Denielson, A., Holland, H.D., (1994): Geology and major and trace element chemistry of late Archean weathering profiles in the Fortescue Group Western Australia: implications for atmospheric pO2. Precambrian Research, 65, 297-317.

Mansour, M. (1994): Sedimentology and radioactivity of Um Bogma Formation, West Central Sinai, Egypt, M.Sc. Thesis, Faculty of Science, Suez Canal Univ., 157 p.

McAlister, J.J. and Smith, B.J., (1997): Geochemical trends in Early Tertiary palaeosols from northeast Ireland: a statistical approach to assess element behaviour during weathering. In: Widdowson, M. (Ed.), Palaeosurfaces: Recognition, Reconstruction and Palaeoenvironmental Interpretation. Geological Society Special Publication, Geological Society, London, 120, 57–65.

McLennan, S.M., (1989): Rare earth elements in sedimentary rocks; influence of provenance and sedimentary processes. In: Lipin, B.R., McKay, G.A. (Eds.), Geochemistry and Mineralogy of Rare Earth Elements. Reviews of Mineralogy, 21, 169-200.

Michel, D., (1983): Les oxy-hydroxydes de fer: Leur rôle dans La distribution de l'uranium dans le milieu supergène. Thèse Nancy, 178p.

Mira, H. I. and Aita, S.K. (2009): Remobilization of uranium and copper through karstification processes; A case study in in Abu Thor locality , Um Bogma region , West Central Sinai, Egypt , Annals Geol. Surv. Egypt. , V.31, P. 21-42.

Mira, H. I., Shata, A. E. and El Balakssy, S. S., (2006): Role of microbial action in concentrating uranium and heavy metals within gibbsite mineralization of Um Bogma area, Southwest Sinai, Egypt: 7th Intern. Conf.Geochem., Fac. Sci., Alex., Egypt, Vol. III, P. 185-203.

Mitchell, R.L., Sheldon, N.D., (2010): The~1100 Ma Sturgeon Falls paleosol revisited: implications for Mesoproterozoic weathering environments and atmospheric CO_2 levels. Precambrian Research, 183, 738-748.

Moustafa, A.M., (1987): Drap folding in the Baba – Sidri area, eastern side of the Suez rift, Egypt, J Geol., 31, 13-24.

Panahi, A., Young, G.M., Rainbird, R.H., (2000): Behaviour of major and trace elements (including REE) during Paleoproterozoic pedogenesis and diagenetic alteration of an Archean granite near Ville Marie, Quebec, Canada. Geochimica et Cosmochimica Acta, 64, 2199-2220.

Railsback, L.B., (2003): An earth scientist's periodic table of the elements and their ions. Geology 31 (9), 737-740.

Rojkova, E.V., Razoumnaia, E.G., Serebriakova, M.B. and Chitcherbak, O.V., (1958): Le rôle de la sorption dans la concentration de l'uranium dans les roches sedimentaries, Conf. sur l'utilisation e l'énergie atomique à des fins pacifiques, ONU Genève, 160-172.

Sharkov, Y.V. and Yakoleva, M.N., (1971): Concerning the origin of higher radioactivity of iron weathering zone. In: Prospecting for Uranium Ore Deposits in Mountain Taija, Atomizdat [in Russian].

Shata, A. E. and Mira, H. I., (2010): Mineralogy and geochemistry of the Mo-U-REE bearing carbonaceous shale in Um Bogma area, southwest Sinai, Egypt. Jour. of Sediment., 18, 7-14.

Sheldon, N.D. and Tabor, N.J., (2009): Quantitative paleoenvironmental and paleoclimatic reconstruction using paleosols. Earth-Science Reviews, 95, 1-52.

Soliman, M.S., (1975): Petrology of Carboniferous dolostone marine transgression over West Central Sinai, Egypt. 7th Int. Congr. Straits. Geol. Carbnonif., C.R. Krefeld, 4: 53-265.Springer Verlag, Berlin, P340.

Van der veijden, C.H., Arthur, R.C. and Langmuir, D., (1974): Sorption of uranyl by hematite. Theoretical and geochemical implications, Geol. Soc. Am. Abs. Prog. Annual meeting, Denver 10.

Wronkiewicz, D.J., Condie, K.C., (1987): Geochemistry of Archean shales from the Witwatersrand Supergroup, South Africa: source-area weathering and provenance. Geochimica et Cosmochimica Acta, 51, 2401-2416.

Zhmodik, S.M., Mironov, A.G. and Nemirovskaya, N.A., (1980): Uranium distribution in iron hydroxides from weathered mantle as shown by F-radiography, Dokl. Akad. Nauk. USSR, 250 6 (1980), 219-222.

Zau, L. and Lin, J., (1996): the geochemical features and evolution of laterite in the karst area of Guizhou province.Chinese Jour. Geo., Vol.15, No., 4, 353-363.

452
453
454
455
456
457
458
459
460
461
462
463
464
465
466
467
468
469
470
471
472